



## Interaction Analysis between Existing Loaded Piles and Braced Excavation Design Parameters

Received 13 January 2023; Revised 25 February 2023; Accepted 13 March 2023

Mohamed G.I. Shaaban<sup>1</sup>  
Mostafa A. Abd El-Naiem<sup>2</sup>  
Abdel-Aziz A. Senoon<sup>3</sup>  
Mamdouh A. Kenawi<sup>4</sup>

### Keywords

Braced excavation.  
Fully saturated sand.  
Finite element method;  
Excavation geometry.  
Design parameters.  
Pile group behavior;  
Settlement

### Abstract

Three-dimensional numerical analyses are conducted using the finite element software PLAXIS 3D to gain insight into the interaction behavior between deep excavation and adjacent piled foundations in fully saturated sand. Effects of excavation width and depth, the distance between strut level and the excavation surface with each excavation stage, strut stiffness, diaphragm wall stiffness, and diaphragm wall depth are examined during the adjacent excavation. In practice, incorrect values of the braced excavation design parameters may result in an uneconomical or even unsafe design. The analyses revealed that increasing the excavation width or depth has a significant influence on the adjacent pile group behavior. Additionally, it is also observed that reducing the distance between the strut level and the excavation surface with each excavation stage, increasing the struts stiffness, increasing diaphragm wall thickness or depth, and reducing the horizontal or vertical span of struts can assist to reduce settlement and tilting of the pile group induced by the adjacent excavation.

## 1. Introduction

Excavation works near existing structures generate concerns related to foundation failure and subsequent structural damage. In most cases, soil settlement induced by excavation cannot be avoided. The adjacent piled structures may be collapsed when the foundation settlement exceeds the allowable value. One of the most famous damage caused by nearby excavation is the collapse of 13-storey building in China in 2009 [1], [2]. Thus, there is an increasing need for studying interaction behaviour between existing piled structures and adjacent excavation. Numerous studies were carried out to investigate excavation-induced horizontal displacement and bending moment in existing piles. Those studies included numerical analyses [3]–[5], centrifuge test [6] and actual full-scale test

<sup>1</sup> Assist. lecturer, Dept. of Civil. Eng., Sohag University, Sohag, Egypt. [mohamed\\_shabanp2@eng.sohag.edu.eg](mailto:mohamed_shabanp2@eng.sohag.edu.eg)

<sup>2</sup> Professor, Dept. of Civil. Eng., Assiut University, Assiut, Egypt. [mostafaabdo6689@gmail.com](mailto:mostafaabdo6689@gmail.com)

<sup>3</sup> Professor, Dept. of Civil. Eng., Assiut University, Assiut, Egypt. [asenoon2000@yahoo.ca](mailto:asenoon2000@yahoo.ca)

<sup>4</sup> - Assoc. professor, Dept. of Civil. Eng., Sohag University, Sohag, Egypt. [mkenawi2@yahoo.com](mailto:mkenawi2@yahoo.com)

[7]. However, excavation-induced settlement and tilting in existing piles were neglected in those studies. Settlement and tilting of a structure are employed in engineering practice to determine the damage potential of structures. Field investigations reported by [8], [9] showed that many buildings supported by pile foundations were damaged by excavation-induced settlement and tilting.

A limited number of studies was performed to investigate pile settlement due to adjacent excavation in dry or unsaturated sandy soil [10]–[15]. Moreover, the settlement and tilting behaviour of a floating pile group adjacent to deep excavation in soft clay was demonstrated by [16]. In addition, a formula for determining the soil settlement induced by excavation in soft clay as a function of depth and surface soil settlement was obtained by [17]. However, the influence of upper structure integrity on pile settlement did not consider. In a thick sand layer, damage to buildings adjacent to an excavation was explored by [18] using PLAXIS 2D. Numerical analyses were conducted by [19] to illustrate the role of sand relative density on an existing piled raft foundation due to twin-excavations. In addition, a series of centrifuge tests and numerical analyses were performed by [20] to investigate impact of double basements construction sequence (i.e., excavated sequentially and simultaneously) on an existing pile group in dry sand. The results indicated that, construction of the double basements simultaneously is safer. An analytical approach was proposed by [21] to predict effect of dewatering on adjacent pile foundations in clay and silty soils. In simplified conditions, pile settlement due to the adjacent excavation can be obtained [22]. However, soil was represented simply as springs and load transferring between the springs is not allowed. Although stiff excavation support system may provide a safety factor against structural damage, it may yield soil movements. In actual analysis, a wrong choice values of the design parameters for braced excavation may lead to an uneconomical or even unsafe design. Considering the lack of a systematic study of excavation-induced effects on adjacent structures in fully saturated sand, this paper seeks to analyse settlement and tilting behaviour of a capped pile groups due to the adjacent deep underwater excavation works. Findings from this study are used to advise engineers on important factors that to be considered during design of deep excavations adjacent to existing deep foundations.

## **2. Three-dimensional finite-element analysis**

### **2.1. Numerical analysis plan**

The complex ground movements and deformations caused by an excavation can be captured by the finite-element method. Finite-element program PLAXIS 3D (CONNECT Edition V20) [23] was employed in the current numerical analysis. Figure 1 shows a typical excavation geometry that was chosen for the analysis. The numerical analysis included a model of existing pile group and multi-stage excavation with a 15 m final depth. The excavation was supported by a concrete diaphragm wall with five levels of struts. The horizontal and vertical spacing of the struts were 8.0 m and 3.0 m, respectively. Analysis was performed to investigate the response of a 2 x 2 pile group subjected to initial vertical applied load and close to an excavation in saturated Berlin sand. The front pair of piles were located at a distance of 3 m from the diaphragm wall. In this study, the centre-to-centre pile spacing was three times of the pile diameter ( $d_p$ ). To avoid soil-cap interaction and the contribution of the cap in load-carrying capacity, an elevated pile group was chosen in this investigation. The elevated pile group reflects the worst-case scenario encountered in engineering

practice. The piles were rigidly connected to the pile cap and the cap was subjected to an initial uniformly distributed load. Dimensions of the pile cap were 3.5 m long  $\times$  3.5 m wide  $\times$  1 m deep. Before the excavation, a numerical simulation of the pile load test for the pile group was carried out. Based on the failure criterion proposed by [24] for bored piles, the ultimate load-carrying capacity of the pile group (i.e., failure load) was obtained to be 677 kN/m<sup>2</sup> and uniformly distributed on the pile cap. By taking a safety factor (FOS) as 2.5, the uniformly applied load on the pile cap before and during the excavation is 270.8 kN/m<sup>2</sup>. In the current study, the effects of excavation width and depth, distance between strut level and the excavation surface with each excavation stage, strut stiffness, diaphragm wall stiffness, and diaphragm wall depth were investigated during the adjacent excavation. A variety of numerical analyses have been performed to look at how piled buildings react to the adjacent excavation, as summarized in Table 1.

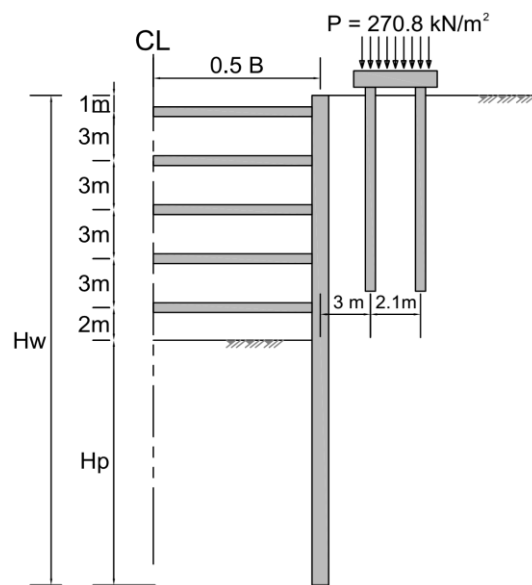


Fig. 1: Excavation geometry of the model

**Table 1.** Parametric study program

Series No.	Parameter studied	Excavation width, B (m)	Excavation depth, He (m)	Distance between strut level and the excavation surface, Y (m)	Strut axial rigidity, EA (kN) $\times 10^6$	Wall thickness, tw (m)	Wall depth, Hw (m)
1	Excavation width and depth	10, 20, 30, 40	1.5, 4.5, 7.5, 10.5, 13.5, 15	0.5	9.03	1.0	30
2	Distance between strut level and the excavation surface	20	1.5, 4.5, 7.5, 10.5, 13.5, 15	0.5, 1.0, 1.5	9.03	1.0	30
3	Strut stiffness	20	1.5, 4.5, 7.5, 10.5, 13.5, 15	0.5	4.515, 6.773, 9.03	1.0	30

Series No.	Parameter studied	Excavation width, B (m)	Excavation depth, He (m)	Distance between strut level and the excavation surface, Y (m)	Strut axial rigidity, EA (kN) x 10 <sup>6</sup>	Wall thickness, tw (m)	Wall depth, Hw (m)
4	Wall stiffness	20	1.5, 4.5, 7.5, 10.5, 13.5, 15	0.5	9.03	0.6, 0.8, 1.0, 1.25, 1.6	30
5	Wall depth	20	1.5, 4.5, 7.5, 10.5, 13.5, 15	0.5	9.03	1.0	30, 32.5, 35, 37.5

**2.2. Finite-element mesh and boundary conditions**

A typical 3D view of the finite element model mesh and boundary conditions adopted in this study are illustrated in Fig. 2. Only half of the excavation width was modelled due to geometrical symmetry. The boundaries are far enough to cause any restriction to the analysis. To analyse ground settlement, the mesh must be extended in the lateral direction (y) to a distance equal to four times the final excavation depth from the wall, as recommended by [25]. In other words, mesh length is just the sum of half excavation width (0.5 B) and four times the final excavation depth (4 He). Based on numerical parametric analysis, the mesh refinement degree was chosen by the criterion that the variation of computed pile group settlement was less than 10% if the size of the current mesh was halved. It is decided to choose a fine mesh-size and the mesh becomes finer for the plates and embedded piles as large shear strain variations were expected. Moreover, the soil elements are relatively small near the excavation and gradually increase in size as they move away from it to maintain a logical balance between the results' accuracy and analysing costs.

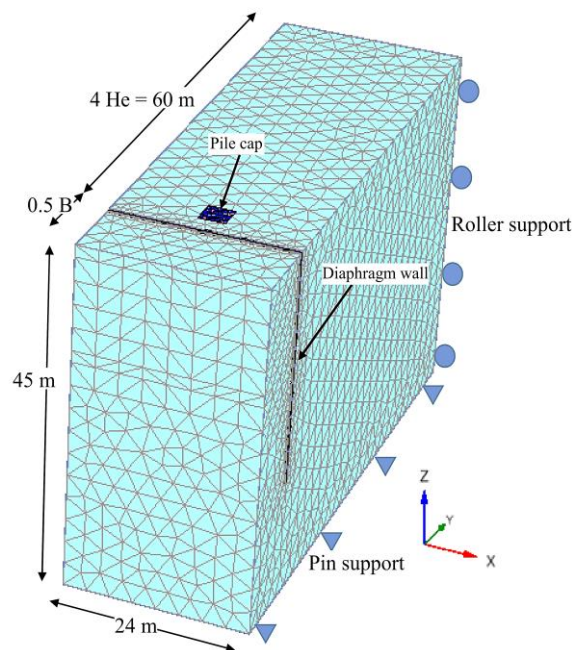


Fig. 2: Finite-element mesh and boundary conditions adopted in this study.

Soil deformations in directions normal to vertical planes are restrained by roller supports but the bottom boundary is fixed by pin supports in all directions. Whereas, the top surface of the model is free in all directions. The soil elements in the mesh were the 10-node tetrahedral elements, while a 6-node plate element was employed to model the behaviour of the pile cap and diaphragm wall. In addition, soil-wall interaction was simulated using 12-node interface elements. The interface element consists of a pair of nodes to ensure that it is compatible with the 6-noded triangular side of the plate element or soil element [23]. Initially, the ground water level was assumed at the ground surface, which developed a hydrostatic initial pore-water pressure profile. All vertical sides and the model's base were simulated without flow conditions, while free drainage was allowed at the mesh's top boundary. The bored piles were simulated using embedded piles with 3-node line elements. The embedded piles behave like volume piles when interacting with soil through special interface elements. It is discovered that the embedded pile model is able to reproduce the behaviour of laterally loaded pile with rough shaft surface in the numerical analysis [26]. Moreover, the formulation of the embedded pile element and its validation are provided in [23], [27], [28]. The Layer dependent option has been used to relate the local skin resistance to the strength properties (cohesion  $c$  and friction angle  $\phi$ ) and the interface strength reduction factor, ( $R_{inter}$ ), as defined for soil layers. Moreover, manual input of maximum skin and base resistances is required instead of being a result of finite element analysis to avoid the undesired high values. The parameters used for the embedded pile element are summarized in Table 2. Struts were simulated in the analysis using fixed-end anchor elements, which are point elements in PLAXIS 3D. The concrete diaphragm wall and pile cap material behaviours were assumed to be linear elastic with a realistic elastic modulus, unit weight, and Poisson's ratio of 30 GPa, 25 kN/m<sup>3</sup>, and 0.2, respectively.

**Table 2.** Material properties of the pile adopted in the finite element analyses.

Parameter	Value
Material type	Elastic
Young's modulus, $E$ (GPa)	30
Pile diameter, $d_p$ (m)	0.7
Pile length, $L_p$ (m)	12
Unit weight, $\gamma$ (kN/m <sup>3</sup> )	25.0
Maximum shaft resistance, $T_{s, max}$ , (kN/m)	78
Maximum base resistance, $F_{max}$ , (kN)	1555

### 2.3. Constitutive model and model parameters

The soil nonlinear behaviour was simulated by using a hardening soil model with small-strain stiffness (HS Small). The most important feature of this constitutive model is the difference between Young's modulus values under loading and unloading conditions. Furthermore, this soil model can simulate different soil reactions from small strains to large strains. Thus, the HS small model could significantly enhance the reliability of deep excavation analysis by providing more accurate displacements after each excavation stage [29], [30]. A reasonable simulation of sand deformations was produced by using 0.95 as the interface strength reduction factor ( $R_{inter}$ ). [28]. The soil parameters are derived from reference solution by [29], [31] and summarized in Table 3. Validation and verification of the Hs small model and soil parameters were available in [29].

**Table 3.** Soil parameters adopted in the finite element analyses.

Parameter	Value
Unit weight above phreatic level, $\gamma_{\text{unsat}}$ (kN/m <sup>3</sup> )	19.0
Unit weight below phreatic level, $\gamma_{\text{sat}}$ (kN/m <sup>3</sup> )	20.0
Triaxial compression stiffness, $E_{50}$ (kN/m <sup>2</sup> )	45000
Primary oedometer stiffness, $E_{\text{oed}}$ (kN/m <sup>2</sup> )	45000
Unloading/reloading stiffness, $E_{\text{ur}}$ (kN/m <sup>2</sup> )	180000
Power for stress-level dependency of stiffness, $m$	0.55
Cohesion, $C'$ (kN/m <sup>2</sup> )	1.0
Friction angle, $\Phi'$ (°)	35.0
Dilatancy angle, $\Psi'$ (°)	5.0
Shear strain at which $G_s = 0.722G_0$ , $\gamma_{0.7}$	0.0002
Shear modulus at very small strains, $G_0^{\text{ref}}$ (kN/m <sup>2</sup> )	168750
Unloading/reloading Poisson's ratio, $\nu_{\text{ur}}$	0.20
Reference stress for stiffness, $P_{\text{ref}}$	100
$K_0$ -value for normal consolidation, $K_0^{\text{nc}}$	0.43
Tensile strength, $\sigma_{\text{tension}}$	0.00
Failure ratio, $R_f$	0.90
Interface strength reduction factor, $R_{\text{inter}}$	0.95

#### 2.4. Numerical modelling procedure

Piles and diaphragm wall were wished-in-place, which means that the behaviour of the pile was close to the bored pile and installation effects were not considered. Since the bottom-up excavation method is widely used, it was chosen for the current study. The bottom-up excavation method is superior to the top-down method in terms of project cost and construction duration. The water table inside the excavation area was lowered until it reached the excavation level with each stage. For every excavation stage in the current study, excavation was sufficiently slow to allow a steady-state flow field situation. This was a valid assumption for relatively slow excavations in high-permeable soils. Water pressure on the passive side is set to zero at the excavation level and the same steady state pressure is developed on both active and passive sides below the diaphragm wall. In engineering practice, the project is divided into phases. Each phase is divided into several calculation steps. This is important because the non-linear behaviour of soil necessitates applying loadings in small proportions. It is interesting to remark that displacements are set to zero before starting the excavation works to exclude deformations due to initial loads and diaphragm wall installation. Staged construction provides an accurate simulation of various loading, construction, and excavation processes. The numerical modelling procedures are summarized as follows:

1. Generation of the initial stresses using  $K_0$  procedure.
2. Construction of pile cap and all embedded piles (wished-in-place pile group).
3. Application of initial working load on the pile cap.
4. Construction of wished-in-place diaphragm wall.
5. Reset displacements to zero, completion of the first excavation stage.
6. Installation of struts at level -1.0 m.
7. Completion of the second excavation stage.
8. Installation of struts at level -4.0 m.

9. Completion of the third excavation stage.
10. Installation of struts at level -7.0 m.
11. Completion of the fourth excavation stage.
12. Installation of struts at level -10.0 m.
13. Completion of the fifth excavation stage.
14. Installation of struts at level -13.0 m.
15. Completion of the last excavation stage.

To evaluate the influence of excavation depth below the struts' location, struts are installed 0.5 m, 1.0 m, and 1.5 m above the excavation surface with each excavation stage. The excavation stages are described in Fig. 3 and Table 4.

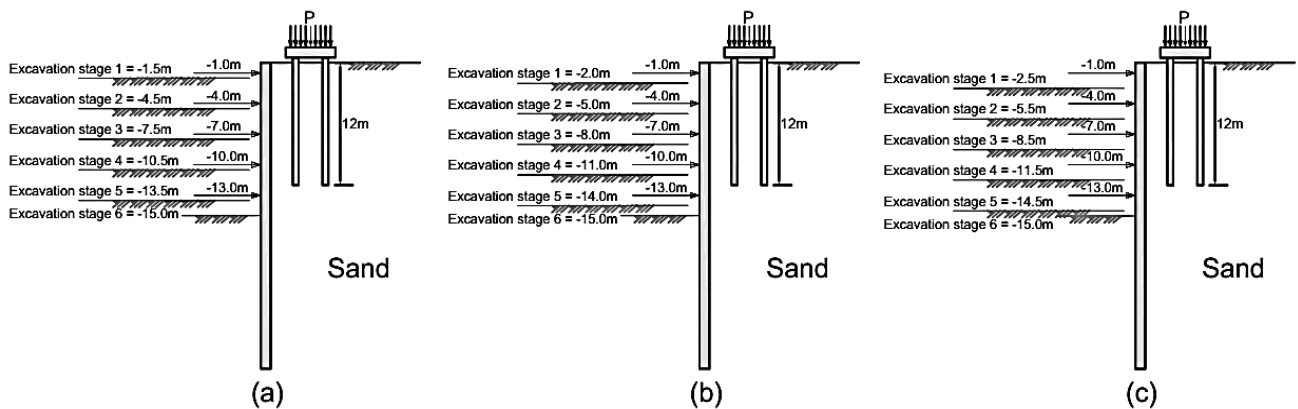


Fig. 3: Excavation stages in cases of (a) 0.5 m, (b) 1.0 m, and (c) 1.5 m distance between the strut and the excavation surface

**Table 4.** Excavation stages in the finite element analyses.

Excavation stages	Distance between strut and excavation surface		
	0.5 m	1.0 m	1.5 m
First excavation stage	Excavation down to level -1.5 m	Excavation down to level -2.0 m	Excavation down to level -2.5 m
Second excavation stage	Excavation down to level -4.5 m	Excavation down to level -5.0 m	Excavation down to level -5.5 m
Third excavation stage	Excavation down to level -7.5 m	Excavation down to level -8.0 m	Excavation down to level -8.5 m
Fourth excavation stage	Excavation down to level -10.5 m	Excavation down to level -11.0 m	Excavation down to level -11.5 m
Fifth excavation stage	Excavation down to level -13.5 m	Excavation down to level -14.0 m	Excavation down to level -14.5 m
Last excavation stage	Excavation down to level -15.0 m	Excavation down to level -15.0 m	Excavation down to level -15.0 m

### 3. Analysis of results

#### 3.1 Effects of the excavation width and depth

Four excavation widths ( $B = 10, 20, 30,$  and  $40$  m) have been considered in this study to explore the influence of excavation geometry on pile group responses with the advancement of excavation. The effect of excavation depth ( $H_e$ ) and width ( $B$ ) on pile group settlement is presented in Fig. 4. Pile group settlement ( $\Delta$ ) and excavation depth ( $H_e$ ) are normalized by the pile diameter ( $d_p$ ) and pile length ( $L_p$ ), respectively. The normalized pile group settlement is presented in percentage units. Pile group settlement is evaluated at the centre of the pile cap with reference to its original elevation. As expected, pile group settlement due to the adjacent excavation increases with increasing the excavation depth. Similar trend of pile settlement during the excavation was observed by [12], [16], [25]. The primary reasons for this settlement are shaft frictional resistance losses as excavation progress and the reduction of pile end-bearing resistance due to excavation closer to level of the pile toe. Moreover, excavation produces large stress relief and causes unbalanced earth pressures on both sides of the diaphragm wall, which produces settlement and tilting of the adjacent structures. Due to increasing the excavation depth from  $13.5$  m to  $15$  m, settlement increases by more than  $100\%$  (i.e., from  $3.57\% d_p$  to  $7.60\% d_p$ ) in the case of  $40$  m excavation width. The pile capacity is frequently obtained from load-settlement curve and the induced settlement can be regarded as an additional load on pile head. Therefore, the existing pile capacity changes during the excavation. The influence of excavation depth and width on pile cap tilting is shown in Fig. 5. Tilting is computed by dividing the differential settlement between two edges of the pile cap by the horizontal distance between them. The pile cap tilting is presented in percentage form. The pile cap tilting increases with increasing excavation width. Tilting towards the excavation is positive; whereas tilting away from the excavation is negative as illustrated in Fig. 5. Tilting starts positively and increases till ( $H_e/L_p = 0.6$ ). While negative pile cap tilting results from further advancement of the excavation. This observation may be attributed to the interaction between front and rear piles and change in effective vertical stress beneath the piles. At the end of the excavation, the maximum pile cap tilting is  $0.2\%$  in the case of  $40$  m excavation width. This value is equal to the maximum allowable tilting, according to [25], [32]. However, a study by [33] found that the building may face the risk of instability when the tilting is equal or greater than  $0.1\%$ .

Deformations of the diaphragm wall increases due to increasing the excavation width [25]. Increasing the excavation width causes a large zone of plastic deformations, which leads to an increase in pile group settlement and tilting. Thus, the designed size of the excavation (excavation depth and width) must be respected, and over-excavation is harmful. The over-excavation process will cause unpredictable amounts of adjacent pile group settlement and tilting. Settlement and tilting of the pile group slightly increase with the increase of excavation width for excavation above the pile toe level (i.e.,  $H_e/L_p < 1.0$ ). However, deeper excavation ( $H_e/L_p > 1.0$ ) gives a faster increased rate of pile group settlement and tilting due to increasing the excavation width. Increasing the excavation width from  $10$  m to  $40$  m results in a little increase in pile group settlement (from  $6.5$  mm to  $10.0$  mm) and pile cap tilting (from  $0.007\%$  to  $0.015\%$ ) at  $10.5$  m excavation depth. However, a significant increase in pile group settlement (from  $14.6$  mm to  $53.2$  mm) and pile cap tilting (from  $0.059\%$  to  $0.2\%$ ) are observed due to increasing the excavation width from  $10$  m to  $40$  m at the end of the excavation (i.e.,  $H_e = 15$  m). When the excavation width is equal to  $40$  m, settlement and tilting of the pile group reach the largest values at the end of the excavation. It is also



implied that the reduction of excavation width reduces the amount of increase in pile group settlement and tilting with the advancement of the excavation.

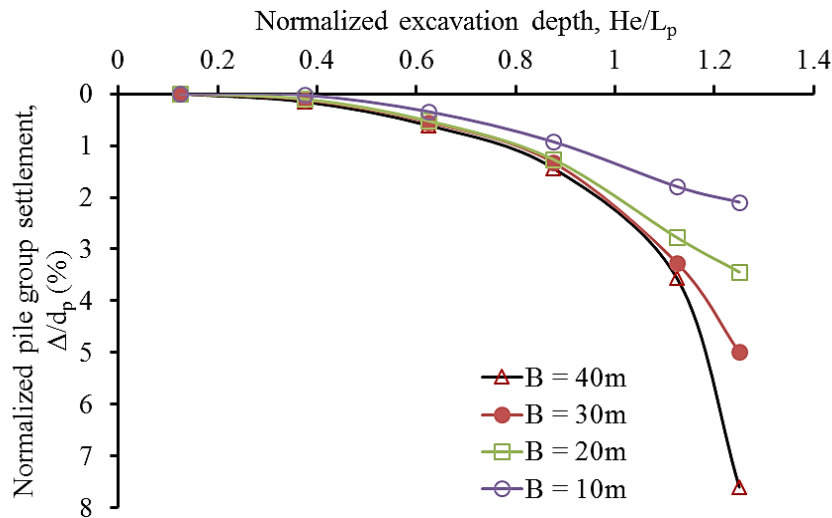


Fig. 4: Effects of excavation depth and width on pile group settlement during the excavation

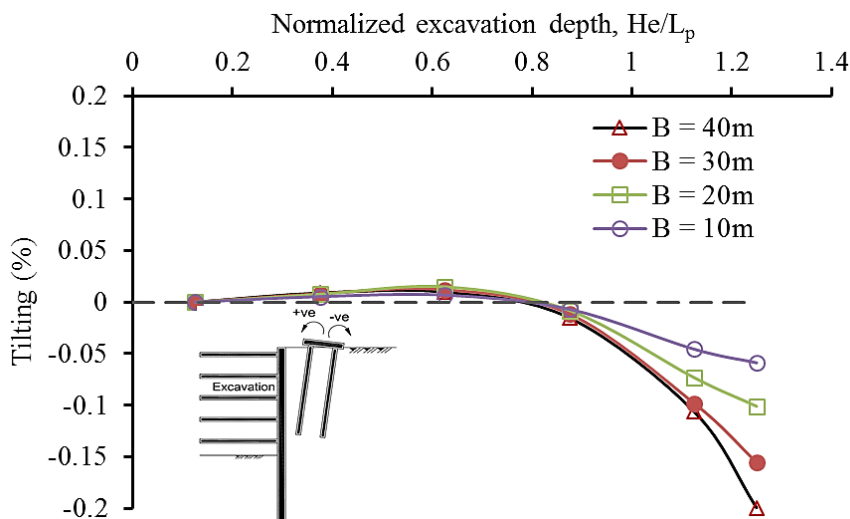


Fig. 5: Effects of excavation depth and width on pile cap tilting during the excavation

### 3.2 Effects of the distance between the strut and the excavation surface

Three tests have been performed to investigate the effects of distance between the strut level and the excavation surface with each excavation stage on pile group responses. All tests have the same wall stiffness, final excavation depth, number of excavation stages, strut spacing, number of strut levels, and location of struts. The only difference between them is the distance between the strut level and the excavation surface with each excavation stage. Struts are installed 0.5 m, 1.0 m, and 1.5 m above the excavation surface in the three tests (See Fig. 3). Unsupported length of the wall refers to the distance between the lowest level of struts and the excavation surface. It can be minimized by decreasing the distance between the strut level and the excavation surface in each excavation stage.

In the first test, struts are installed 0.5 m above the excavation surface. The unsupported length of the wall is 1.5 m after completing the first excavation stage (i.e., the excavation depth reaches 1.5 m). Due to installation of the first level of struts at level -1.0 m and the excavation depth reaches 4.5 m (i.e., after completing the second excavation stage), the unsupported length of the wall is 3.5 m. Struts are installed 1.0 m above the excavation surface in the second test. After reaching 2.0 m excavation depth (i.e., after finishing the first stage of excavation), the unsupported length of the wall is 2.0 m. Whereas, after struts installation at level -1.0 m and reaching 5.0 m excavation depth (i.e., after finishing the second stage of excavation), the unsupported length of the wall is 4.0 m. In the third test, struts are installed 1.5 m above the excavation surface. After completing the first excavation stage (i.e., the excavation depth reaches 2.5 m), the unsupported length of the wall is 2.5 m. However, the unsupported length of the wall is 4.5 m after installation of struts at level -1.0 m and completing the second excavation stage (i.e., the excavation depth reaches 5.5 m). Results in Fig. 6 show the incremental pile group settlement with the advancement of excavation in the cases of 0.5 m, 1.0 m, and 1.5 m distance between the strut level and the excavation surface. Deep excavation necessarily causes settlement and soil movements close to the excavation site. The total settlement of the adjacent pile group is the accumulated settlement at every stage of the excavation. Thus, settlement and deformations increase by increasing the distance between the strut level and the excavation surface with each excavation stage. It can be observed that the pile group experiences a significant increase in settlement with increasing the distance between the strut level and the excavation surface when the excavation level is located below the pile toe (i.e.,  $H_e/L_p > 1.0$ ). Generally, the wall unsupported length and soil deformations in the case of 0.5 m distance are smaller than those in the other distances. The maximum pile group settlement increases by approximately 87% (i.e., from 3.44%  $d_p$  to 6.43%  $d_p$ ) when the distance increases from 0.5 m to 1.5 m. In the same way, the maximum settlement increases by approximately 53% (i.e., from 4.20%  $d_p$  to 6.43%  $d_p$ ) when the distance increases from 1.0 m to 1.5 m.

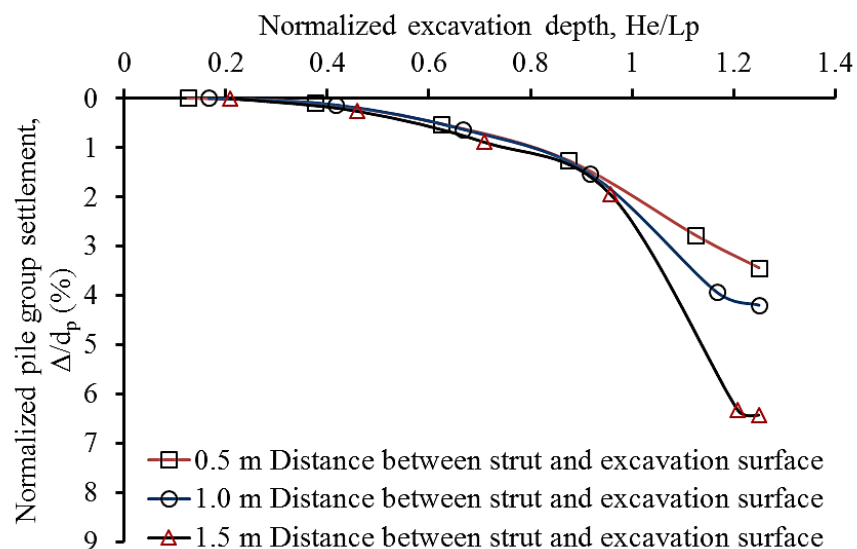


Fig. 6: Effect of the distance between the strut and the excavation surface on pile group settlement during the excavation

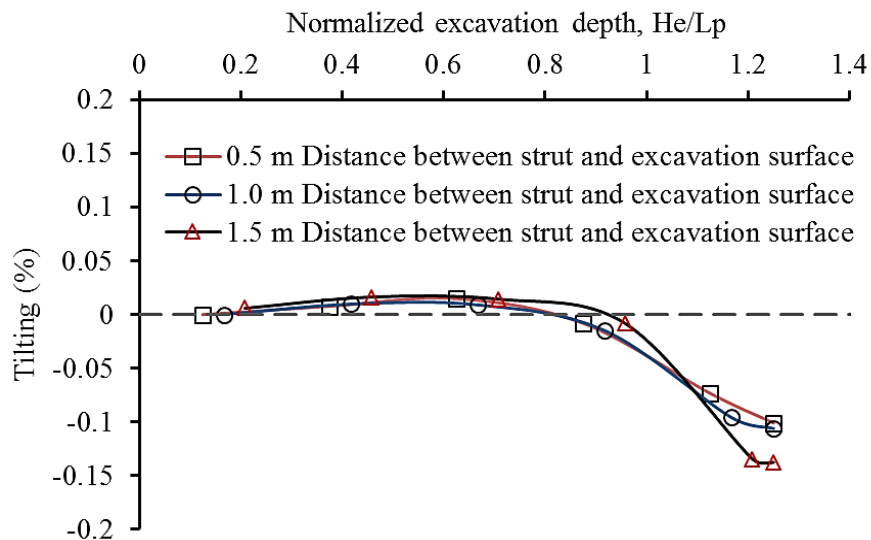


Fig. 7: Effect of the distance between the strut and the excavation surface on pile cap tilting during the excavation

Variations of pile cap tilting for the different distances between the strut level and the excavation surface with each excavation stage are presented in Fig. 7. General trend of the pile group tilting is noted to be similar for the three tests. Tests with 0.5 m and 1.0 m distances have the same tilting of the pile group at the start and the end of excavation; however, 1.5 m distance shows a difference in pile group tilting. Additionally, maximum tilting in the pile group increases with increasing the distance between the strut and the excavation surface. At the end of excavation, the pile cap tilting is 0.10%, 0.11%, and 0.14% corresponding to 0.5 m, 1.0 m, and 1.5 m distance, respectively. This can be attributed to the higher rate of soil movements in case of high distance from strut to excavation surface and high wall unsupported length at deeper excavation.

### 3.3 Effects of strut stiffness

Increasing the stiffness of struts per unit width can be achieved by increasing strut cross-sectional area or decreasing horizontal spacing between the struts. Figures 8 and 9 demonstrate the effects of strut axial rigidity ( $EA$ ) on pile group settlement and tilting during the excavation, respectively. Results show that the stiffness of the strut has a considerable impact on pile group settlement at the end of the excavation. It can be seen that if the strut stiffness is higher, the pile group experiences lower settlement and tilting due to the lower soil movements during the excavation. In the case of strut axial rigidity equal to  $4.52 \times 10^6$  kN, tilting of the pile group is 0.13% at the end of excavation (i.e.,  $He = 15$  m). The strut stiffness has a major impact on pile group settlement and tilting in case of deeper excavation (i.e.,  $He/L_p > 1.0$ ). However, the strut stiffness has a minor impact on the settlement and tilting when the excavation is carried out above the pile toe level (i.e.,  $He/L_p < 1.0$ ).

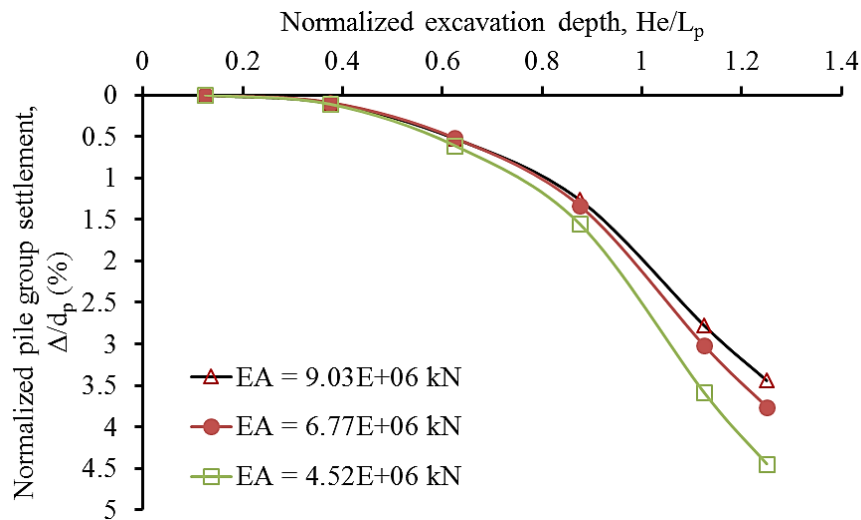


Fig. 8: Effect of strut axial rigidity on pile group settlement during the excavation

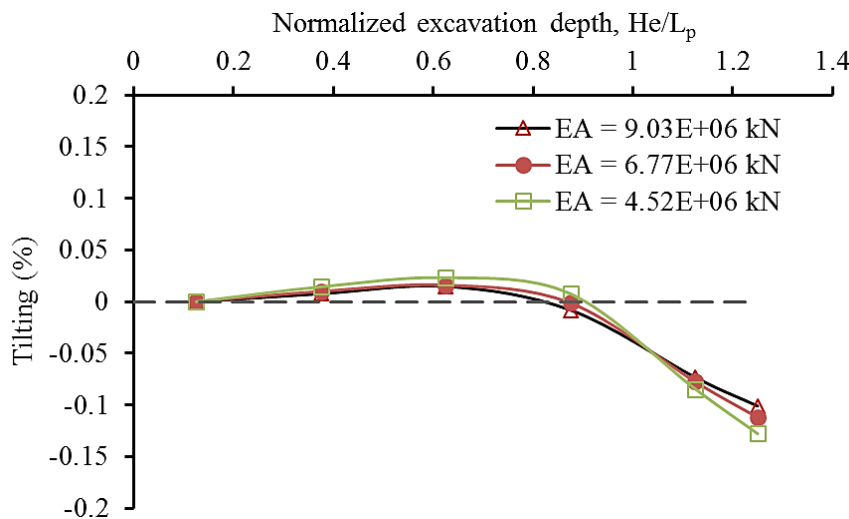


Fig. 9: Effect of strut axial rigidity on pile cap tilting during the excavation

### 3.4 Effects of diaphragm wall stiffness

The support system stiffness can be raised by increasing the diaphragm wall thickness or decreasing the vertical spacing between the struts. Five different values of the wall thickness ranging from 0.6 m to 1.6 m are considered in this study to investigate the effects of wall thickness on pile group responses to the adjacent excavation. Figure 10 shows the effect of the wall thickness on the pile group settlement at various excavation depths. A similar pattern of pile settlement during the excavation was observed by [10], [16]. When the stiffness of the support system is increased by 8 times (by doubling the wall thickness), the pile group settlement decreases by up to 55% (i.e., from 4.50%  $d_p$  to 2.02%  $d_p$ ) at the end of excavation (i.e.,  $H_e = 15$  m). In the same way, the pile group settlement decreases by 61% when the thickness of the wall is doubled corresponding to 10.5 m excavation depth. This is because adjacent excavation causes smaller soil deformation and stress relief when the wall thickness is large enough. In the case of 0.6 m wall thickness, pile group settlement is 6.42%  $d_p$  at the end of the excavation. This value exceeds the maximum allowable settlement (5.12%  $d_p$ ), according to the failure criterion proposed by [24].

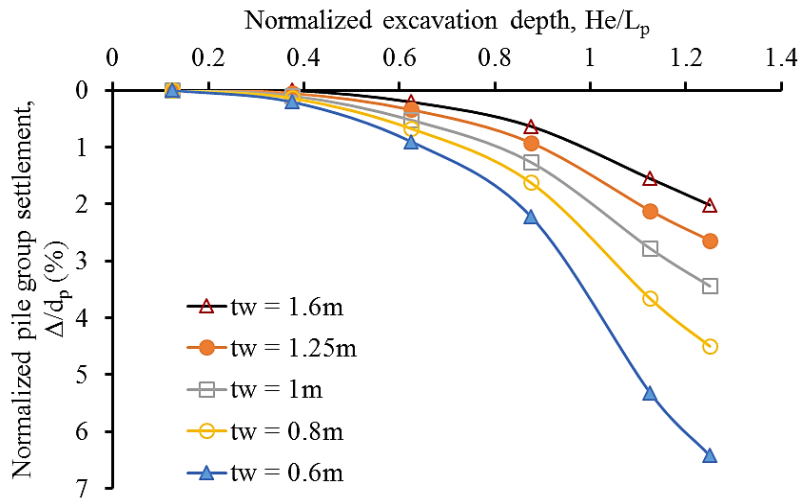


Fig. 10: Effect of diaphragm wall thickness on pile group settlement during the excavation

During the excavation, the influence of diaphragm wall thickness on pile cap tilting is displayed in Fig. 11. The analysis confirms that the pile cap tilting is reduced with the increase in the wall thickness. Moreover, the influence of the wall thickness is more noticeable when the excavation depth reaches 15 m. The same observation was made by [16]. At end of the excavation, the amount of pile cap tilting drops from 0.13% to 0.06% due to increasing the support system stiffness by 8 times. It can be established that the provision of high supporting system stiffness (i.e., high diaphragm wall thickness) would help to moderate the pile group settlement and tilting.

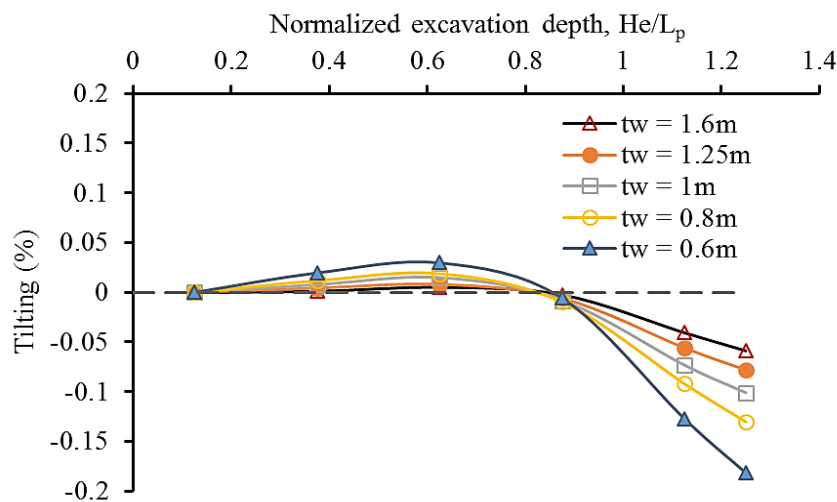


Fig. 11: Effect of diaphragm wall thickness on pile cap tilting during the excavation

### 3.5 Effects of diaphragm wall depth

The diaphragm wall needs to be embedded sufficiently deep below the final excavation level to maintain stability. Results in Fig. 12 show the influence of wall depth ( $H_w$ ) on the pile group settlement during the excavation. A negligible difference in the pile group settlement is observed with an increase of wall embedded depth when the excavation depth is relatively small (i.e.,  $H_e \leq 10.5$  m). At deeper excavation (i.e.,  $H_e = 13.5$  m and 15 m), it is noted that the pile group settlement can be reduced by increasing the wall depth from 30 m to 32.5 m (i.e., increasing the ratio of wall penetration depth to excavation depth from 1.0 to 1.17 reduces pile group settlement when the

excavation depth is large). However, reduction in the settlement is limited with an increase of the wall embedment depth when the wall depth is greater than 32.5 m (i.e.,  $H_w/H_e \geq 2.4$ ). To minimize the construction cost and material waste, it is recommended to support excavation in saturated sand by multi-strutted diaphragm wall with an embedded depth equal or smaller than 1.4 times the excavation depth. The influence of wall depth on pile cap tilting during the excavation is plotted in Fig. 13. It can be observed that the tilting is reduced due to increasing the wall depth in case of deeper excavation (i.e.,  $H_e/L_p > 1.0$ ). The pile cap tilting is reduced from 0.10% to 0.07% when the wall depth varies from 30 m to 37.5 m at the end of the excavation.

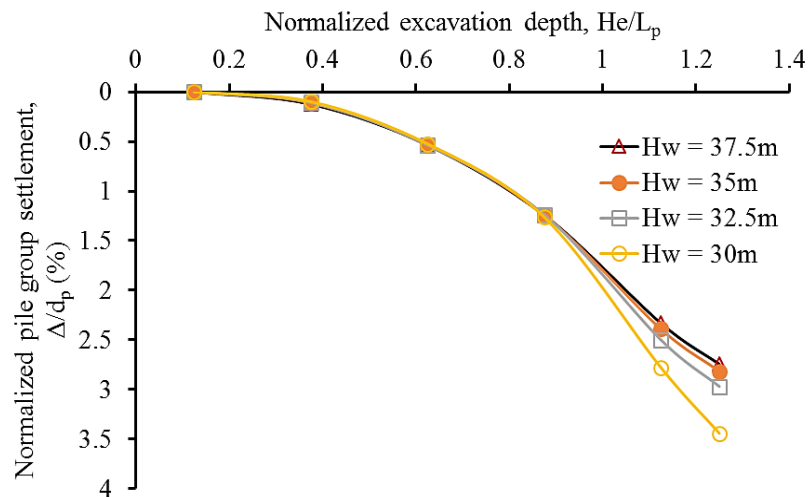


Fig. 12: Effect of diaphragm wall depth on pile group settlement during the excavation

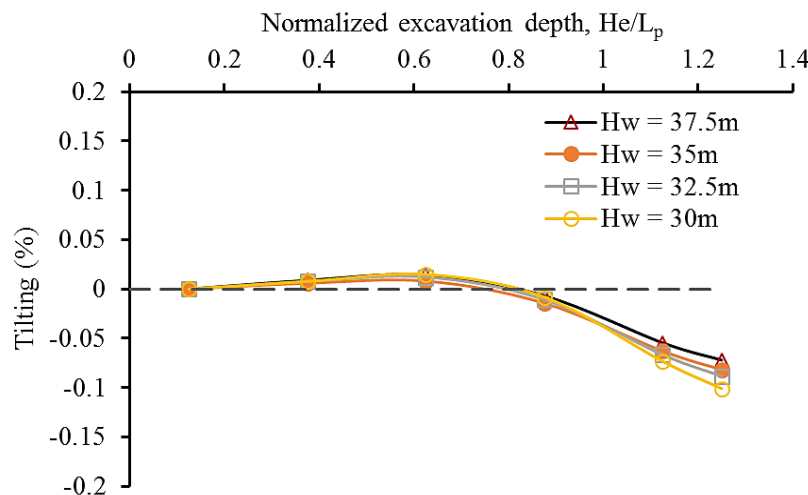


Fig. 13: Effect of diaphragm wall depth on pile cap tilting during the excavation

#### 4. Conclusions and recommendations

In this study, an extensive numerical parametric study was carried out to investigate the interaction behaviour between existing loaded piles and braced excavation design parameters in saturated sand. Based on the obtained results, the following conclusions may be drawn:

1. Pile group settlement increases with increasing the excavation depth. Moreover, increasing the excavation width causes a large zone of plastic deformations, which leads to an increase in pile group settlement and tilting. Thus, it is important to avoid over-excavation.
2. The pile group experiences a significant increase in settlement and tilting with increasing distance between the strut level and the excavation surface with each excavation stage when the excavation level is located below the pile toe (i.e.,  $H_e/L_p > 1.0$ ). Therefore, excavation depth beneath the struts should be minimal with each excavation stage.
3. The induced pile group settlement and tilting can be reduced by increasing the strut axial rigidity due to the lower soil movements during the excavation.
4. The provision of high supporting system stiffness (i.e., high diaphragm wall thickness) would help to moderate the pile group settlement and tilting. Moreover, the influence of wall thickness is more significant at deeper excavation.
5. When the excavation depth is relatively small, a negligible difference in the pile group settlement is observed with an increase of wall embedded depth. At deeper excavation, it is noted that the pile group settlement and tilting can be reduced by increasing the ratio of wall penetration depth to excavation depth. However, negligible change in pile settlement is observed when the ratio of wall penetration depth to excavation depth is more than 1.4. Therefore, it is recommended to support excavation in saturated sand by multi-strutted diaphragm wall with embedded depth equal or smaller than 1.4 times the excavation depth.

In this study, all numerical analyses of deep underwater excavation works are performed on sandy soils. Any extrapolation from these findings should be treated with caution. Effect of excavation on multi-layered soil with different supporting systems may be considered in further analyses.

## References

- [1] W.-D. Wang, C. W. W. Ng, Y. Hong, Y. Hu, and Q. Li, "Forensic study on the collapse of a high-rise building in Shanghai: 3D centrifuge and numerical modelling," *Géotechnique*, vol. 69, no. 10, pp. 847–862, 2019.
- [2] W. Wang, Q. Li, and Y. Hu, "Collapse of a high-rise building with pretensioned high-strength concrete piles," *Proc. Inst. Civ. Eng. - Forensic Eng.*, vol. 173, no. 1, pp. 3–12, Feb. 2020, doi: 10.1680/jfoen.19.00012.
- [3] R. Zhang, W. Zhang, and A. T. C. Goh, "Numerical investigation of pile responses caused by adjacent braced excavation in soft clays," *Int. J. Geotech. Eng.*, pp. 1–15, 2018.
- [4] M. G. Shaikhoun, "Interaction behavior between existing building piles and piles supporting excavation (M. Sc. Thesis)," 2017.
- [5] R. Zhang, A. T. C. Goh, and W. Zhang, "3D numerical analysis of passive pile groups adjacent to deep braced excavation in soft clay," *J. ISSN TBA*, vol. 3, 2020.
- [6] D. E. Ong, C. E. Leung, and Y. K. Chow, "Pile behavior due to excavation-induced soil movement in clay. I: Stable wall," *J. Geotech. Geoenvironmental Eng.*, vol. 132, no. 1, pp. 36–44, 2006.
- [7] A. T. C. Goh, K. S. Wong, C. I. Teh, and D. Wen, "Pile Response Adjacent to Braced Excavation," *J. Geotech. Geoenvironmental Eng.*, vol. 129, no. 4, pp. 383–386, Apr. 2003, doi: 10.1061/(ASCE)1090-0241(2003)129:4(383).
- [8] M. Korff, *Response of piled buildings to the construction of deep excavations*, vol. 13. IOS Press, 2013.
- [9] Y. Tan, R. Huang, Z. Kang, and W. Bin, "Covered semi-top-down excavation of subway station surrounded by closely spaced buildings in downtown Shanghai: Building response," *J. Perform. Constr. Facil.*, vol. 30, no. 6, p. 4016040, 2016.
- [10] J. Shi, J. Wei, C. W. W. Ng, and H. Lu, "Stress transfer mechanisms and settlement of a floating pile

- due to adjacent multi-propped deep excavation in dry sand,” *Comput. Geotech.*, vol. 116, p. 103216, Dec. 2019, doi: 10.1016/j.compgeo.2019.103216.
- [11] M. A. Soomro, N. Mangi, W.-C. Cheng, and D. A. Mangnejo, “The Effects of Multipropped Deep Excavation-Induced Ground Movements on Adjacent High-Rise Building Founded on Piled Raft in Sand,” *Adv. Civ. Eng.*, vol. 2020, pp. 1–12, Oct. 2020, doi: 10.1155/2020/8897507.
- [12] C. W. W. Ng, M. Shakeel, J. Wei, and S. Lin, “Performance of Existing Piled Raft and Pile Group due to Adjacent Multipropped Excavation: 3D Centrifuge and Numerical Modeling,” *J. Geotech. Geoenvironmental Eng.*, vol. 147, no. 4, p. 4021012, Apr. 2021, doi: 10.1061/(ASCE)GT.1943-5606.0002501.
- [13] H. Karira, A. Kumar, T. H. Ali, D. A. Mangnejo, and N. Mangi, “A parametric study of settlement and load transfer mechanism of piled raft due to adjacent excavation using 3D finite element analysis,” *Geomech. Eng.*, vol. 30, no. 2, pp. 169–185, 2022, doi: 10.12989/gae.2022.30.2.169.
- [14] C. W. W. Ng, J. Wei, H. Poulos, and H. Liu, “Effects of Multipropped Excavation on an Adjacent Floating Pile,” *J. Geotech. Geoenvironmental Eng.*, vol. 143, no. 7, p. 04017021, Jul. 2017, doi: 10.1061/(ASCE)GT.1943-5606.0001696.
- [15] R. Feng, Q. Zhang, and S. Liu, “Experimental Study of the Effect of Excavation on Existing Loaded Piles,” *J. Geotech. Geoenvironmental Eng.*, vol. 146, no. 9, p. 4020091, 2020.
- [16] M. Shakeel and C. W. W. Ng, “Settlement and load transfer mechanism of a pile group adjacent to a deep excavation in soft clay,” *Comput. Geotech.*, vol. 96, pp. 55–72, Apr. 2018, doi: 10.1016/j.compgeo.2017.10.010.
- [17] Y.-Y. Liang, N.-W. Liu, F. Yu, X.-N. Gong, and Y.-T. Chen, “Prediction of Response of Existing Building Piles to Adjacent Deep Excavation in Soft Clay,” *Adv. Civ. Eng.*, vol. 2019, pp. 1–11, Dec. 2019, doi: 10.1155/2019/8914708.
- [18] Q. T. Huynh, T. Boonyatee, and S. Keawsawasvong, “Behavior of a Deep Excavation and Damages on Adjacent Buildings: a Case Study in Vietnam,” *Transp. Infrastruct. Geotechnol.*, pp. 1–29, 2020.
- [19] H. Karira, A. Kumar, T. H. Ali, D. A. Mangnejo, and L. Yaun, “Numerical investigation of responses of a piled raft to twin excavations: Role of sand density,” *Geomech. Eng.*, 2022, doi: 10.12989/gae.2022.31.1.053.
- [20] J. Shi et al., “Effects of construction sequence of double basement excavations on an existing floating pile,” *Tunn. Undergr. Sp. Technol.*, vol. 119, p. 104230, Jan. 2022, doi: 10.1016/j.tust.2021.104230.
- [21] Y. Liu, B. Xiang, and M. Fu, “Influence of Dewatering in Deep Excavation on Adjacent Pile Considering Water Insulation Effect of Retaining Structures,” *Geotech. Geol. Eng.*, vol. 37, no. 6, pp. 5123–5130, 2019.
- [22] M. Korff, R. J. Mair, and F. A. F. Van Tol, “Pile-Soil Interaction and Settlement Effects Induced by Deep Excavations,” *J. Geotech. Geoenvironmental Eng.*, vol. 142, no. 8, p. 04016034, Aug. 2016, doi: 10.1061/(ASCE)GT.1943-5606.0001434.
- [23] R. B. J. Brinkgreve, L. Zampich, and N. R. Manoj, “PLAXIS 3D CONNECT Edition V20 tutorial manual,” *Delft Univ. Technol. PLAXIS bv, Netherlands*, 2019.
- [24] C. W. W. Ng, T. L. Y. Yau, J. H. M. Li, and W. H. Tang, “New Failure Load Criterion for Large Diameter Bored Piles in Weathered Geomaterials,” *J. Geotech. Geoenvironmental Eng.*, vol. 127, no. 6, pp. 488–498, Jun. 2001, doi: 10.1061/(ASCE)1090-0241(2001)127:6(488).
- [25] C.-Y. Ou, *Deep excavation: theory and practice*. CRC Press, 2006.
- [26] T. P. T. Dao, “Validation of PLAXIS embedded piles for lateral loading (M. Sc. Thesis),” 2011.
- [27] F. Tschuchnigg and H. F. Schweiger, “The embedded pile concept – Verification of an efficient tool for modelling complex deep foundations,” *Comput. Geotech.*, vol. 63, pp. 244–254, Jan. 2015, doi: 10.1016/j.compgeo.2014.09.008.
- [28] I. Al-aboodi and T. T. Sabbagh, “Numerical Modelling of Passively Loaded Pile Groups,” *Geotech. Geol. Eng.*, vol. 37, no. 4, pp. 2747–2761, Aug. 2019, doi: 10.1007/s10706-018-00791-z.
- [29] T. Benz, “Small-strain stiffness of soils and its numerical consequences (Ph. D. Thesis),” Stuttgart, Inst. f. Geotechnik., 2007.
- [30] Y.-M. Hsieh, P. H. Dang, and H.-D. Lin, “How Small Strain Stiffness and Yield Surface Affect Undrained Excavation Predictions,” *Int. J. Geomech.*, vol. 17, no. 3, p. 04016071, Mar. 2017, doi: 10.1061/(ASCE)GM.1943-5622.0000753.
- [31] H. F. Schweiger, “Results from numerical benchmark exercises in geotechnics,” in *Proc. 5th European Conf. Numerical Methods in Geotechnical Engineering (P. Mestat, ed.)*, Presses Ponts et



*chaussees, Paris*, 2002, pp. 305–314.

- [32] L. M. Zhang and A. M. Y. Ng, “Probabilistic limiting tolerable displacements for serviceability limit state design of foundations,” *Géotechnique*, vol. 55, no. 2, pp. 151–161, Mar. 2005, doi: 10.1680/geot.55.2.151.59527.
- [33] C. Xu, K. Yang, X. Fan, J. Ge, and L. Jin, “Numerical Investigation on Instability of Buildings Caused by Adjacent Deep Excavation,” *J. Perform. Constr. Facil.*, vol. 35, no. 5, p. 4021040, 2021.

## تحليل التفاعل بين الخوازيق المحملة القائمة ومعاملات تصميم الحفر المسنود

يتم في هذه الدراسة إجراء التحليلات العددية ثلاثية الأبعاد باستخدام برنامج العناصر المحدودة PLAXIS 3D لاكتساب نظرة على السلوك التفاعلي بين الحفر العميق والأساسات الخازوقية المجاورة في التربة الرملية المشبعة بالماء. إن تأثيرات عرض وعمق الحفر، والمسافة بين مستوى الدعامات وسطح الحفر في كل مرحلة من مراحل الحفر، وجساءة الدعامات، وجساءة الحائط الساند، وعمق الحائط الساند تم تفسيرها جميعاً أثناء الحفر المجاور للأساسات الخازوقية. وقد تؤدي القيم غير الصحيحة لمعاملات تصميم الحفر المسنود إلى تصميم غير اقتصادي أو حتى غير آمن. كما كشفت التحليلات أن زيادة عرض أو عمق الحفر له تأثير واضح على سلوك مجموعة الخوازيق المجاورة للحفر. وعلاوة على ذلك، تم ملاحظة أن تقليل المسافة بين مستوى الدعامات وسطح الحفر في كل مرحلة من مراحل الحفر، وزيادة جساءة الدعامات، وزيادة سمك أو عمق الحائط الساند، وتقليل المسافات الأفقية أو الرأسية بين الدعامات يمكنها جميعاً المساعدة في تقليل هبوط وميول مجموعة الخوازيق المجاورة للحفر.